Secretory Autophagy via VMP1-Containing Extracellular Vesicles in Pancreatic Stress Responses

Mariana S. Tadic[1], Felipe J. Renna[1], Malena Herrera López[1], Fabiana López Mingorance[1], Tamara Orquera[1], Diego A. Chiappetta[2], Alejandro Ropolo[1], Maria I. Vaccaro[1]*

[1] Universidad de Buenos Aires - CONICET, Instituto de Bioquímica y Medicina Molecular Prof Alberto Boveris (IBIMOL), Buenos Aires, Argentina.

[2] Universidad de Buenos Aires, Instituto de Tecnología Farmacéutica y Biofarmacia (InTecFyB), Buenos Aires, Argentina.

- *Correspondence: maria.vaccaro@gmail.com

Abstract

Cellular stress activates mechanisms such as autophagy and vesicular trafficking to maintain homeostasis in pathological conditions like acute pancreatitis. One such mechanism involves the unconventional secretion of extracellular vesicles (EVs). Vacuole Membrane Protein 1 (VMP1), an autophagy-related protein implicated in pancreatitis, diabetes, and pancreatic cancer, triggers autophagy through ubiquitination and interaction with BECN1. Here, we demonstrate that VMP1 is secreted into the extracellular medium and incorporated into EV membranes. Using cell lines expressing VMP1-tagged plasmids, we isolated VMP1-containing EVs (VMP1-EVs) via ultracentrifugation and immunoisolation. Additionally, VMP1-EVs are internalized by recipient cells. VMP1-EV secretion decreased with mTOR inhibition and in Atg5-deficient cells. In pancreatic acinar cells, endogenous VMP1 secretion increased under

stress conditions, including blocked autophagic flux and experimental pancreatitis. In a rat model of pancreatitis, VMP1 secretion in pancreatic juice was increased. TEM and DLS analyses revealed that VMP1-EVs have a diameter of approximately 150 nm. Immunoprecipitation assays confirmed that LC3-II is secreted in VMP1-EVs, with secretion enhanced under lysosomal blockade. Moreover, VMP1 downregulation reduced the secretion of LC3 and p62, indicating that VMP1 is required for their release. This study provides the first evidence that VMP1 is secreted via a secretory autophagy pathway as a component of EVs. Understanding VMP1-mediated secretory autophagy may offer new insights into the clinical relevance of EVs in pancreatic diseases.

Keywords: Acute Pancreatitis; ATG5; Autophagosome; Bafilomycin A1; LC3; Lysosomal Stress; Membrane Protein; p62; Pancreatic Cells; Pancreatic Juice

Abbreviations

AP: Acute Pancreatitis

Arg: Arginine

BafA1: Bafilomycin A1

CM: conditioned medium

DLS: Dynamic Light Scattering

EVs: Extracellular Vesicles

empty GFP: pEGFP-N1

FLAG–Ubiquitin: FLAG.Ub

GFP: Green Fluescent Protein

LC3: Microtubule-associated protein 1 light chain 3

p62: SQSTM1/p62 (sequestosome 1)

Pancreatic Juice: PJ

PBS: Phosphate-buffered saline

SA: Secretory autophagy

TEM: Transmission electron microscopy

VMP1: Vacuole Membrane Protein 1

$VMP1^{\Delta Atg}$: construct lacking the C-terminal 18 amino acids of VMP1 (residues 388–406).

VMP1-EVs: VMP1-containing EVs

VMP1.FLAG-EVs: VMP1.FLAG-containing EVs

VMP1.FLAG: pLenti–hVMP1–FLAG

VMP1.GFP: pEGFP-N1-hVMP1

VMP1.GFP-EVs: VMP1.GFP-containing EVs

VMP1 KD: *VMP1* knockdown

VMP1.V5: pcDNA4-B–hVMP1–V5/His

WCL: whole cell lysate

WT: Wild-Type

Introduction

Macroautophagy/autophagy is a tightly regulated catabolic process that mediates the selective degradation of damaged or superfluous cellular components, thereby preserving cellular homeostasis and promoting survival under stress [1]. While autophagy is classically regarded as a degradative pathway, accumulating evidence has expanded its functional repertoire to include non-canonical roles in secretion. This has led to the recognition of secretory autophagy (SA) [2], a process in which autophagic components are repurposed for unconventional secretion, encompassing the release of leaderless cytosolic proteins, secretory lysosomes, and extracellular vesicles (EVs) [2,3]. EVs are membrane bound vesicles secreted by cells into the extracellular space. EVs exhibit diverse sizes, contents, and surface markers [4,5].

Despite advances in our understanding of SA, the precise molecular mechanisms underlying this process remain incompletely defined. Autophagy and endosomal trafficking are mechanistically intertwined, sharing membrane sources, regulatory proteins, and vesicular dynamics. Autophagy related proteins - including ATG5, LC3 (microtubule-associated protein 1 light chain 3) and SQSTM1/p62 (sequestosome 1). - participate in both degradative and secretory events [6,7]. These intersections highlight the broader role of autophagy beyond lysosomal degradation, extending to vesicle-mediated intercellular communication.

SA is increasingly recognized as a key contributor to diverse pathophysiological conditions, including inflammation, cancer, neurodegeneration, and metabolic diseases [8]. It is typically induced under stress conditions such as nutrient deprivation, endoplasmic reticulum (ER) stress, and accumulation of misfolded proteins that trigger the unfolded protein response (UPR) [9]. Under these circumstances, components normally targeted for lysosomal degradation may instead be secreted through autophagy-dependent mechanisms.

Vacuole Membrane Protein 1 (VMP1) is a 406–amino acid transmembrane protein first identified through the search for genes differentially expressed in pancreatitis [10]. In a series of previous studies, we demonstrated that VMP1 expression alone is sufficient to induce autophagy in mammalian cells under nutrient-rich conditions, through direct binding of its carboxy-terminal peptide to the BH3 domain of BECN1 [11,12]. Briefly, upon expression, VMP1 is ubiquitinated and interacts with BECN1, thereby facilitating the recruitment of the PI3KC3 (Class III phosphatidylinositol 3-kinase) complex I to sites of autophagosome formation at endoplasmic reticulum–plasma membrane contact points. VMP1 subsequently becomes an integral component of the autophagosome membrane [11–14]. Beyond its role in bulk autophagy, VMP1 is critically important in cellular responses to disease. Its expression is undetectable in the healthy human and murine pancreas but is markedly induced in response to pancreatitis [11,15], pancreatic cancer [16–18], and diabetes [19]. Under stress conditions associated with acute pancreatitis (AP), VMP1 expression triggers zymophagy-the selective autophagic degradation of activated zymogen granules [20], as well as mitophagy-the selective removal of damaged mitochondria [21], playing a protective role and avoiding the progression of pancreatitis to severe disease [22]. The regulation of VMP1 is complex, involving transcriptional and post-translational control. We previously described transcriptional programs involving AKT1–GLI3 and E2F1–EP300 that regulate VMP1 expression [16,18], and more recently, identified VMP1 as a target of CRL4/Cdt2-mediated ubiquitination in pancreatic cancer cells, a modification required for its recruitment to the autophagosome [14].

Given VMP1 localization to autophagosomal membranes and its induction under stress, we hypothesized that VMP1 may also participate in SA. In the present study, we provide the first evidence that VMP1 is secreted via EVs and incorporated into their membrane structure. This secretion is regulated by autophagy and is enhanced under stress conditions such as lysosomal inhibition and experimental pancreatitis. The discovery of this alternative secretory pathway

may advance our understanding of VMP1 function in health and disease and open new avenues for investigating autophagy-dependent secretion in the context of pancreatic injury and beyond.

Materials and Methods

Animal Model of AP

AP was induced in male and female Wistar rats (8–10 weeks old) with Arginine (Arg) by intraperitoneal injection of L-arginine hydrochloride, a well-established model of pancreatic injury mediated by metabolic and oxidative stress. Animals received two i.p. injections of 250 mg Arg per 100 g body weight, prepared as a 20% solution in sterile saline (pH adjusted to 7.0), with a 1 h interval between doses. Rats had *ad libitum* access to food and water between injections. Animals were euthanized at indicated time points for histological and biochemical analysis of pancreatic tissue. Control animals received equivalent volumes of sterile saline following the same injection schedule. All animal procedures were approved by the Animal Care and Research Committee of the School of Pharmacy and Biochemistry, University of Buenos Aires (REDEC 2024 1664 E UBA DCT FFYB), and were conducted in accordance with the International Guiding Principles for Biomedical Research Involving Animals.

Cell Culture, Transfections, and Differentiation

HEK293T, HeLa, MIA PaCa-2 and AR42J cell lines were obtained from the American Type Culture Collection. Wild-type (WT) and *Atg5*-knockout MEFs were generously provided by Dr. María I. Colombo (Universidad Nacional de Cuyo, CONICET, Argentina). MIAPaCa-2 pancreatic cancer cells with stable knockdown of VMP1, achieved via shRNA expression, and vector control cells were used to evaluate VMP1 expression. All cell lines were cultured in Dulbecco's Modified Eagle Medium (Biological Industries) supplemented with either 10% or 20% fetal bovine serum (Natocor), 200 mM L-alanyl-L-glutamine dipeptide (Gibco™), 100

U/mL penicillin, and 100 μg/mL streptomycin (Biological Industries). Cells were maintained at 37°C in a humidified 5% CO_2 incubator. Mycoplasma contamination was routinely assessed by DAPI staining (monthly) and by PCR (biannually). HEK293T cells were transfected at 60–70% confluence using polyethyleneimine (Polysciences, cat. no. 24765-1). Culture medium was replaced with fresh conditioned medium (CM) 5 h post-transfection. AR42J cells were differentiated by incubation with 100 nM dexamethasone for 48 h prior to experimental procedures.

Treatments

For amino acid deprivation, cells were washed twice with fasting medium (140 mM NaCl, 1 mM $CaCl_2$, 1 mM $MgCl_2$, 5 mM glucose, 1% BSA, and 20 mM HEPES, pH 7.4) and incubated in the same medium for 16 h to collect CM. PP242 (Santa Cruz Biotechnology) was dissolved in DMSO to prepare a 1 mM stock solution, and cells were treated with 1 μM PP242 for 16 h. Chloroquine diphosphate (Sigma-Aldrich) was dissolved in phosphate-buffered saline (PBS) to obtain a 10 mM stock solution; cells were treated with 50 μM chloroquine for 16 h. Bafilomycin A1 (Santa Cruz Biotechnology; cat. no. sc-201550A) was prepared as a 10 μM stock solution in DMSO and applied at final concentrations, according to cell types, of 10 nM, 20 nM or 100 nM for 16 h. For hyperstimulation of cholecystokinin receptors, differentiated AR42J cells were treated with 7.4 μM caerulein (Sigma-Aldrich) for 16 h.

Expression Vectors

The plasmids pEGFP-N1-hVMP1 (VMP1.GFP), pcDNA4-B–hVMP1–V5/His (VMP1.V5), and pLenti–hVMP1–FLAG (VMP1.FLAG) were generated as previously described in Renna et al., 2023 [14]. The pLKO.1-Puromycin vector containing a pre-designed shRNA sequence targeting human VMP1 (5′-GCAATGAACAAGGAACATCAT-3′; catalog number RHS3979-

98821402) was used to generate MIAPaCa-2 *VMP1* knockdown (*VMP1* KD) cells. A deletion construct lacking the C-terminal 18 amino acids of VMP1 (residues 388–406), termed VMP1$^{\Delta Atg}$, was cloned into the pENTR1A-GFP-N2 vector (Addgene plasmid #19364) using BamHI and EcoRI restriction sites, based on the human *VMP1* reference sequence (NM_030938.5). This entry clone was recombined with the pLenti PGK puro destination vector (Addgene plasmid #19068) using Gateway™ LR Clonase™ II enzyme mix (Thermo Fisher Scientific; cat. no. 11791-020). All constructs generated in this study were verified by DNA sequencing. The FLAG–Ubiquitin (FLAG.Ub) plasmid was generously provided by Dr. Simona Polo (University of Milan). We used pEGFP-N1 (empty GFP) as a control.

Generation of Conditioned Culture Medium

To generate exosome-depleted CM, DMEM (Biological Industries) supplemented with 200 mM L-alanyl-L-glutamine dipeptide (Gibco™) and 30% Fetal Bovine Serum (Natocor) was ultracentrifuged at 120,000 × g for 16 h using a Beckman XL-90 ultracentrifuge. The resulting supernatant was filtered through 0.22 µm pore-size filters and transferred to sterile containers. Penicillin (100 U/mL) and streptomycin (100 µg/mL) (Biological Industries) were added to the filtered medium.

Isolation of EVs from Conditioned Culture Medium

CM was collected and subjected to a series of differential centrifugation steps to remove cells and debris: 300 × g for 15 min, followed by 2,000 × g for 20 min at 4°C. The supernatant was then centrifuged at 16,500 × g for 20 min at 4°C. Subsequently, the supernatant was ultracentrifuged at 120,000 × g for 2 h at 4 °C using a Beckman XL-90 ultracentrifuge. The resulting pellet was washed with cold PBS and ultracentrifuged again at 120,000 × g for 1.5 h

at 4°C. The final EV pellet was resuspended in PBS and used for downstream applications, including immunoblotting, immunofluorescence, or immunoprecipitation.

Isolation of EVs from Rat Pancreatic Juice

Pancreatic juice (PJ) collected from experimental animals was centrifuged at 300 × g for 10 min at 4°C, followed by 2,000 × g for 10 min at 4°C to remove cellular debris. The supernatant was then centrifuged at 10,000 × g for 30 min at 4°C. This fraction was diluted in PBS and subjected to ultracentrifugation at 100,000 × g for 2 h at 4°C using a TFT 80.2 rotor in a Sorvall WX+ Ultra Series ultracentrifuge (Thermo Scientific). The pellet was washed with PBS and subjected to a second ultracentrifugation step at 100,000 × g for 1.5 h at 4°C. The final EV pellet was resuspended in PBS for subsequent immunoblotting analysis.

Immunoblot Analysis

Following treatments and transfections, cells were lysed in buffer containing 50 mM Tris-HCl (pH 7.4), 250 mM NaCl, 25 mM NaF, 2 mM EDTA, 0.1% Triton X-100, and protease inhibitors (Thermo Scientific™ Pierce). EV pellets were lysed in the Laemmli buffer. For LC3 detection, cells were lysed in 50 mM Tris-HCl (pH 8.0), 150 mM NaCl, 1% Triton X-100, and protease inhibitors. Protein concentration was quantified using the BCA assay (Pierce), and equal amounts of protein were resolved by SDS-PAGE and transferred to polyvinylidene fluoride (PVDF) membranes (0.22 μm pore size; Millipore). Membranes were blocked in Odyssey Blocking Buffer (LI-COR) for 1 h at rooatgm temperature and incubated overnight at 4°C with the appropriate primary antibodies. Primary antibodies included: anti-VMP1 (N-terminal) (1:1,000; rabbit mAb #12978, Cell Signaling Technology), anti-VMP1 (C-terminal) (1:1,000; rabbit mAb #12929, Cell Signaling Technology), anti-actin (1:2,000; rabbit polyclonal A2066, Sigma–Aldrich), anti-DYKDDDDK tag (1:6,000; mouse mAb #8146, Cell

Signaling Technology), anti-α-tubulin (1:4,000; mouse mAb T5168, Sigma–Aldrich), anti-SQSTM1/p62 (1:1,000; rabbit mAb #8025, Cell Signaling Technology), anti-CD63 (1:1,000; mouse mAb ab231975, Abcam), anti-GFP (1:500; mouse monoclonal antibody 3E6, Invitrogen), anti-ATG5 (1:1000; rabbit monoclonal, #12994, Cell Signaling Technology) and anti-V5 (1:5000; mouse monoclonal, R960-25, Invitrogen). After primary antibody incubation, membranes were washed four times with PBS containing 0.1% Tween-20 (PBS-T), then twice with PBS. Membranes were then incubated for 2 h at room temperature with secondary antibodies: IRDye® 680LT goat anti-rabbit IgG (1:15,000) or IRDye® 800CW goat anti-mouse IgG (1:10,000; LI-COR), diluted in Odyssey Blocking Buffer. Following incubation, membranes were washed again and visualized using the Odyssey® SA system (LI-COR). For LC3 detection, membranes were blocked for 1 h at room temperature in 1% bovine serum albumin (BSA) in TBS containing 0.1% Tween-20 (TBS-T), then incubated with anti-LC3B (1:500; rabbit mAb #3868, Cell Signaling Technology) for 24 h at 4°C. Membranes were washed, then incubated with HRP-conjugated anti-rabbit IgG (1:2,500; Amersham NA934, GE Healthcare) in 1% BSA in TBS-T. Detection was performed using Pierce ECL Plus (Cat# 32134, Thermo Scientific) and visualized on a cDigit Blot Scanner (LI-COR). Band intensities were quantified using FIJI software. Densitometry values were normalized to actin and expressed as the mean ± SEM from three independent experiments.

Immunoprecipitation Assays

For anti-FLAG immunoprecipitation, EV pellets obtained by ultracentrifugation of conditioned culture media were resuspended in 300 µL of 1× PBS and transferred to 2 mL Eppendorf tubes. Samples were incubated with anti-FLAG® M2 magnetic beads (Sigma-Aldrich) for 2 h at 4°C with gentle agitation. Beads were then washed five times with PBS containing 0.02% Tween-20. Proteins were eluted by adding Laemmli buffer followed by heating at 95°C for 5 min. For

anti-GFP immunoprecipitation, Pierce™ Protein G magnetic beads (Invitrogen) previously attached to the Green Fluorescent Protein (GFP) tag antibody (A-11120) were used. EV pellets were resuspended in 300 μL of 1× PBS and incubated with the beads for 1 h at 4°C with agitation. Beads were washed five times with PBS containing 0.02% Tween-20. VMP1.GFP-EVs were eluted by adding Laemmli buffer and heating at 95°C for 5 min.

Fluorescence Intensity of VMP1.GFP-EVs

HEK293T cells transfected with the VMP1.GFP plasmid were cultured, and conditioned media were collected and subjected to ultracentrifugation to isolate EVs. The resulting pellet was resuspended in PBS, and GFP fluorescence was quantified using a SpectraMax i3x microplate reader (Molecular Devices) at 510 nm. The normalized fluorescence intensity of VMP1.GFP-EVs was calculated using the formula: FI_EVs / FI_WCL, where FI_EVs represents the fluorescence intensity of EVs and FI_WCL represents the intensity of the corresponding whole cell lysate (WCL) from VMP1.GFP-transfected cells.

Dynamic Light Scattering (DLS)

DLS measurements were performed on EV pellets obtained from conditioned media of HEK293T cells transfected with the pLenti-Puro-PGK-hVMP1 plasmid. Measurements were carried out at 25°C using a Zetasizer Nano-ZSP system (Malvern Instruments, UK) equipped with a 633 nm He-Ne laser and a ZEN5600 digital correlator.

Transmission Electron Microscopy (TEM)

Following immunoprecipitation of VMP1.FLAG-EVs, samples were resuspended in PBS and fixed with 2% glutaraldehyde in 0.1 M phosphate buffer at 4°C. A small volume of the fixed sample was placed on a 200-mesh copper grid coated with LR white resin membrane (Sigma-Aldrich, L9774), washed eight times with ultrapure water (2 min each), and stained with 2%

aqueous uranyl acetate (pH 7) for 3 min. Excess stain was removed with blotting paper, and grids were air-dried for 15 min at room temperature. Imaging was performed on a Zeiss 109T transmission electron microscope operated at 80 kV, and images were acquired using a Gatan ES1000w digital camera.

Immunofluorescence

Cells were cultured on 15 mm round glass coverslips placed in 12-well plates. A total of 60,000 HeLa or 80,000 AR42J cells were seeded per well. The following day, cells were transfected with the indicated plasmids, if required, and subsequently incubated with control EVs or VMP1 containing EVs for 24 h. After treatment, cells were fixed with 3.6% paraformaldehyde in PBS for 20 min (followed by permeabilization with 0.1% Triton X-100 in PBS for 5 min), or with cold methanol for 6 min in the specific case of LC3 immunofluorescence [23]. Samples were then washed three times with PBS and blocked with 1% BSA in PBS for 1 h at room temperature. Coverslips were incubated overnight at 4°C in a humidified chamber with primary antibodies diluted in blocking solution. The following antibodies were used: anti-FLAG (1:500; mouse mAb, DYKDDDDK Tag (9A3), Cell Signaling Technology), anti-VMP1 (1:1000; rabbit mAb #12929, Cell Signaling Technology), anti-tubulin (1:1000; mouse mAb T5168, Sigma-Aldrich) and anti-LC3 (1:1000, rabbit mAb #3868, Cell Signaling Technology) . After incubation, coverslips were washed three times with PBS and incubated with Alexa Fluor-conjugated secondary antibodies (Alexa Fluor 488, 594, or 647; 1:800, Molecular Probes) for 2 h at room temperature in PBS with 1% BSA. Coverslips were mounted with polyvinyl alcohol (PVA) containing DABCO mounting medium. Confocal images were acquired using a Zeiss LSM 880 confocal microscope equipped with 20× (NA 0.8) and 63× (NA 1.4) Plan-Apochromat objectives.

Quantification of LC3 Dots per Cell

The number of LC3 dots per cell in immunofluorescence images was obtained using the *Find Maxima* tool in Fiji (ImageJ 1.54f, open-source software).

In Vivo Fluorescence Imaging of VMP1.GFP-EVs

HEK293T cells transfected with VMP1.GFP were used to generate EVs by ultracentrifugation of conditioned media. The EV-containing pellet was resuspended in PBS, and a drop of the suspension was placed on a microscope slide, covered with a glass coverslip, and sealed with nail polish. Samples were immediately imaged using a Zeiss LSM 880 confocal microscope with 20× or 63× Plan-Apochromat objectives.

Protease Protection Assay

VMP1.FLAG-EVs were isolated by differential centrifugation and resuspended in 60 µL PBS. The suspension was divided into three aliquots and incubated with: (i) PBS alone, (ii) 100 µg/mL trypsin in PBS, or (iii) 1% Triton X-100 with 100 µg/mL trypsin in PBS. Reactions were carried out for 30 min at 37°C with gentle mixing. Protease activity was halted by adding protease inhibitor cocktail and 2× Laemmli sample buffer. Samples were then subjected to immunoblotting.

Statistical Analysis

All quantitative data are presented as mean ± SEM. Representative images are shown from at least three independent experiments. Statistical analyses were performed using GraphPad Prism 8, as described in the corresponding figure legends.

Results

1. VMP1 is secreted into the cell culture medium via EVs

To determine whether VMP1 is secreted via EVs, CM from HEK293T cells was subjected to differential ultracentrifugation to isolate the EV-enriched pellet. CD63 was used as an EV-fraction marker (Figure 1A). Cells transfected with VMP1.GFP exhibited a clear GFP signal in the EV fraction by immunoblotting, whereas no signal was detected in EVs from cells transfected with an empty GFP vector (Figure 1B).

Confocal microscopy of the EV pellet confirmed the presence of VMP1.GFP-positive vesicles with diameters <1 μm (Figure 1C), and fluorescence quantification corroborated enrichment in VMP1.GFP-expressing cells but not in controls (Figure 1D). Similar results were obtained when cells were transfected with VMP1.V5 or VMP1.FLAG constructs, confirming that secretion was independent of the fusion tag (Figures 1E, F). These results demonstrate that VMP1 is secreted into the extracellular space via EVs.

2. VMP1 is localized to the membrane of VMP1-containing EVs (VMP1-EVs)

Given that VMP1 is a transmembrane protein localized to the autophagosomal membrane, we hypothesized that it retains as a membrane associated protein in EVs. A protease protection assay on EV fractions from VMP1.GFP-expressing cells showed that trypsin treatment of intact EVs abolished the full-length VMP1.GFP signal (~70 kDa), leaving a ~25 kDa GFP fragment detectable with anti-GFP antibodies (Figure 2A), indicating C-terminal exposure of GFP on the EV surface.

VMP1.FLAG-EVs were immunoprecipitated using anti-FLAG magnetic beads from HEK293T cell CM. TEM of the eluates revealed vesicular structures 110–200 nm in diameter (Figure 2B, C). DLS confirmed a homogeneous size distribution (Figure 2D). These data

demonstrate that VMP1 is embedded in the EV membrane with its C-terminal domain facing outward.

3. VMP1–EVs are internalized by recipient cells

To test whether VMP1–EVs can be taken up by recipient cells, VMP1.GFP–EVs from HEK293T cells were incubated with HeLa cells. Confocal microscopy revealed intracellular GFP signals, consistent with EV uptake by recipient HeLa cells (Figure 3A). Similarly, incubation of HeLa cells with CM from VMP1.FLAG-expressing HEK293T cells followed by immunolabeling with anti-FLAG and anti-VMP1 antibodies confirmed internalization (Figure S1). We also examined uptake in the pancreatic cell line AR42J and results are shown in Figure 3B. AR42J cells incubated with VMP1.FLAG-EVs showed intracellular vesicular localization by Z-stack confocal microscopy combined with α-tubulin staining. Moreover, HeLa cells were incubated with vesicular fractions containing VMP1-EVs secreted from HEK293T cells expressing VMP1.GFP, and immunofluorescence for LC3 was performed in the recipient cells. Notably, a significant increase in LC3 recruitment was observed in HeLa cells incubated with VMP1-EVs (Figure 3C). These findings confirm that VMP1-EVs can be internalized by recipient cells and suggest that they may exert a biological effect.

4. VMP1 secretion depends on autophagy

Given VMP1's essential role in autophagy, we examined whether its secretion is regulated by mTOR signaling. Nutrient starvation or PP242 treatment of VMP1.FLAG-expressing HEK293T cells reduced VMP1.FLAG secretion in EVs (Figure 4A). In contrast, chloroquine treatment increased VMP1.FLAG secretion, linking VMP1 release to autophagic flux. (Figure 4B).

Using the autophagy-deficient mutant VMP1$^{\Delta Atg}$.GFP, which is retained in the ER, we found no secretion into EV fractions (Figure 4C, D), indicating that autophagosome formation is required. To further link VMP1 secretion to autophagy, VMP1.FLAG–positive EVs were immunopurified from cells treated with BafA1 A1 . BafA1 increased LC3-II content within VMP1.FLAG EVs (Figure 4E), indicating enrichment of autophagic cargo under lysosomal inhibition. The corresponding immunoblots of WCL are shown in Figure. S2.

Finally, given that VMP1 is ubiquitinated early in autophagosome formation and remains ubiquitinated throughout autophagy, EVs from cells co-expressing VMP1.GFP and FLAG.Ub were immunoisolated using anti-GFP beads. Ubiquitinated VMP1 was detected in EVs from VMP1.GFP and FLAG-Ub coexpressing cells (Figure 4F), consistent with secretion during autophagy.

5. Endogenous VMP1 secretion requires autophagosome formation and is induced by lysosomal inhibition

We tested whether lysosomal inhibition stimulates endogenous VMP1 secretion and whether autophagosome formation is required. In WT MEFs, BafA1 treatment increased VMP1 secretion into EV fractions, whereas *Atg5* KO MEFs displayed markedly reduced VMP1-EV release (Figure 5A).

Given that lysosomal stress enhances p62 secretion via SA, we assessed whether VMP1 contributes to this process in MIA PaCa-2 cells. In VMP1-expressing cells, BafA1 induced secretion of LC3-II and p62 in EV fractions (Figures 5B–D). *VMP1* KD markedly reduced secretion of both proteins, indicating VMP1's role in stress-induced release of autophagy-related cargos.

6. VMP1 secretion is upregulated in pancreatic acinar cells under lysosomal stress and experimental acute pancreatitis

Differentiated AR42J cells treated with BafA1 exhibited increased VMP1 secretion into EV fractions, accompanied by elevated LC3 and p62 levels (Figure 6A), indicating activation of SA under lysosomal stress in pancreatic cells.

In a cellular model of acute pancreatitis (AP) induced by caerulein (CAE, 7.4 μM), EV fractions from treated AR42J cells contained higher VMP1 and LC3-II levels than untreated controls, paralleling increased VMP1 expression in WCL (Figure 6B).

In vivo, EV fractions from pure PJ of Arg-induced AP rats showed significantly higher VMP1 levels than controls (Figure 6C). These findings reveal a SA pathway in which VMP1 is released via EVs in response to pancreatic stress, with potential pathophysiological relevance in AP.

Discussion

Autophagy is a tightly regulated catabolic process that enables the selective degradation of dysfunctional or superfluous cellular components, thereby maintaining cellular homeostasis. While autophagy is classically recognized for its role in cytoplasmic quality control, recent studies have elucidated other non-canonical functions, including participation in secretory pathways collectively termed SA [2]. These pathways encompass both conventional and unconventional protein secretion, the release of EVs, and secretory lysosome exocytosis [24,25].

Here, we demonstrate that VMP1, an autophagy-related transmembrane protein, is secreted within the EV fraction as an integral membrane component. VMP1 secretion is modulated by the autophagic status, being increased by lysosomal blockade and reduced by mTOR inhibition.

It requires the expression of the core autophagy protein ATG5, and VMP1-EVs also carry LC3-II, indicating their co-secretion within the same vesicles. We further show that VMP1-EVs can be internalized by recipient cells, and that VMP1 expression critically influences the secretion of the autophagy-related proteins LC3 and p62. These findings identify VMP1 as a novel contributor to SA. Moreover, we show that different stressors induce VMP1 secretion in pancreatic acinar cells, and that acute pancreatitis in rats promotes the release of VMP1-EVs into PJ, underscoring a key link between VMP1 secretion and the cellular response to acute pancreatitis.

VMP1 was detected in the EV fraction irrespective of the tag or promoter used for expression (Figure 1), including when expressed under a strong promoter, such as CMV in pEGFP and pcDNA4-B plasmids or a moderate promoter, such as PGK in the pLenti plasmid. Moreover, endogenous VMP1 was also detected in the EV fraction, and its levels increased during cellular stress (Figures 5 and 6). The presence of VMP1 as part of the EV fraction is a completely novel discovery that is consistent with the previous discovery of other autophagic proteins as part of EVs: LC3, ATG16L1, LAMP2 [26,27], p62, NBR1, WIPI2 and OPTN [28].

Regarding the size of these VMP1-EVs, using confocal microscopy we visualized GFP-tagged VMP1-EVs (VMP1.GFP-EVs) in conditioned medium, with sizes consistent with EVs (<1 μm; Figure 1). TEM and DLS further confirmed a homogeneous EV population, ranging from 110 to 200 nm (Figure 2). These data are consistent with those EV diameters described in MISEV2023 guidelines [4].

VMP1 is a transmembrane protein [Dusetti et al., 2002] localized to the autophagosomal membrane [Grasso et al., 2011; Renna et al., 2023]. As expected from its topology during autophagosome biogenesis, our results show that VMP1 is embedded in the EV membrane. Protease protection assays and TEM analyses of immunopurified VMP1-EVs confirmed that

the protein's hydrophilic C-terminus peptide is exposed on the EV surface (Figure 2), suggesting a novel role of VMP1 as an EV-integrated membrane protein.

EVs, defined by their diverse protein cargo, function as versatile mediators of intercellular communication. Their protein composition is central to determining biological function: surface receptors and ligands regulate vesicle distribution, interactions with recipient cells or the extracellular matrix, and the initiation of downstream signaling. These effects may occur through direct receptor engagement at the plasma membrane or following vesicle internalization [29,30]. Here, we show that VMP1-EVs are internalized by recipient cells, including HeLa and AR42J cells (Figure 3), and that this uptake promotes LC3 recruitment, supporting their role in intercellular communication as SA vesicles. Although we observed that VMP1-EVs are internalized and trigger autophagy, the precise mechanisms underlying this process remain unclear, including how these vesicles enter recipient cells, whether they engage specific receptors, and how they initiate the autophagic response. Further studies will be required to elucidate these mechanisms.

Mechanistically, the secretion of overexpressed tagged VMP1 was reduced upon inhibition of mTOR by both the pharmacological agent PP242 and starvation (Figure 4). Our results are consistent with previous findings showing decreased EV output under such conditions [31,32].On the other hand, inhibition of lysosomal degradation using chloroquine enhanced the secretion of overexpressed VMP1. This observation is consistent with previous findings in which treatment with chloroquine increases EV secretion [33] and, in particular, of autophagy-related proteins [34]. In addition, we found that endogenous VMP1 secretion in EVs also increases upon inhibition of lysosomal degradation, in this case with BafA1 A1 (Figure 5), which is in agreement with previous reports describing BafA1 A1 as an enhancer of EV secretion [35,36]. The secretion of VMP1, an autophagy-related protein, was found to depend on ATG5, a core component of the autophagy machinery. VMP1 secretion was significantly

reduced in *Atg5*-deficient cells, in line with other studies showing that EV secretion depends on ATG5 expression [8,37,38]. Moreover, by immunoprecipitation, we detected LC3-II in VMP1-EVs, further supporting the notion that components of the autophagic machinery are directly associated with these vesicles and may contribute to their biogenesis and release. As a whole, these results indicate a clear relationship between VMP1 secretion and the autophagy machinery, suggesting that VMP1-EVs are released by a SA pathway.

Supporting the hypothesis of VMP1 being part of a novel SA pathway, we build on prior work showing that the C-terminal domain of VMP1 is required for autophagic flux [11,12]. In line with this, VMP1$^{\Delta Atg}$.GFP was not detected in EVs (Figure 4), indicating that the C-terminus is likewise necessary for entry into the secretory route. Moreover, we recently showed that VMP1 is ubiquitinated during autophagy [14]. Notably, here we find that VMP1 is also ubiquitinated when associated with EVs, reinforcing a mechanistic connection—and potential crosstalk—between autophagy and VMP1–EV secretion. Notably, we found that VMP1 is not only incorporated into EVs, but its expression also positively influences the secretion of two autophagy-related proteins, LC3 and p62 (Figure 5). Under lysosomal blockade conditions induced by BafA1 A1, the secretion of LC3 and p62 was significantly reduced in VMP1 KD cells, indicating that VMP1 contributes to the release of these autophagic proteins. A schematic model illustrating the proposed pathway of SA involved in VMP1-EV secretion according to the main findings of this manuscript is shown in **Figure 7**.

Importantly, SA is activated by a variety of cellular stressors, including endoplasmic reticulum (ER) stress, accumulation of misfolded proteins, and impaired intracellular trafficking—conditions closely linked to the pathogenesis of AP [9,39,40]. In AP, premature activation of digestive zymogens within pancreatic acinar cells initiates a cascade of tissue injury and inflammation. We previously demonstrated that VMP1 is markedly upregulated in pancreatic

acinar cells during AP, where it promotes zymophagy—a selective form of autophagy that mitigates zymogen-induced cytotoxicity—and mitophagy, thereby preserving cellular energy homeostasis and preventing progression to a severe disease [20–22]. In the current study, we demonstrate that AP-mimicking conditions in pancreatic acinar cells induce a significant increase in VMP1 expression in WCL and, importantly, stimulate its secretion via EVs (Figure 6). Moreover, we investigated VMP1 secretion in vivo using a widely accepted animal model of acute pancreatitis [41], in which we previously reported the upregulation of VMP1 in pancreatic acinar cells [15]. Here, VMP1 was detected in the EV fraction isolated from PJ. Also, following Arg-induced AP in rats, VMP1 secretion was significantly increased, confirming the induction of its secretion under pathological conditions. These findings reveal a novel secretory role for VMP1 in response to pancreatitis-associated stress and highlight its potential relevance in pancreatic disease (Figure 8).

In summary, we provide the first evidence that the autophagy-related transmembrane protein VMP1 is secreted via EVs through a SA pathway. VMP1-EV secretion is induced under conditions of lysosomal blockade and pancreatitis-associated stress and is dependent on autophagy. Our findings suggest that VMP1 not only mediates the degradation of damaged components through selective macroautophagy but also participates in non-canonical autophagic processes, including SA via EVs. This dual role may contribute to cellular adaptation and survival during stress and may be particularly relevant in the context of inflammatory diseases such as acute pancreatitis. Understanding the regulation and function of VMP1 secretion could open new avenues for assessing disease severity and for developing diagnostic strategies as well as more rational therapeutic interventions targeting SA pathways.

Author Contributions: Conceptualization, MIV, MST and FJR; methodology, MST, MIV, FJR, MHL, and FLM; validation, MIV and FJR; formal analysis, MST MIV, FJR, AR;

investigation, MST, FJR, MHL, FLM, AR, TO and DAC; funding acquisition and resources AR and MIV; data curation, FJR and AR; writing—original draft preparation, MST, FJR and MIV.; visualization, MST, FJR and MIV.; supervision, MIV, FJR and AR; project administration, MIV. All authors have read and agreed to the published version of the manuscript.

Funding: This work was supported by grants from: Consejo Nacional de Investigaciones Científicas y Técnicas (CONICET) [PIP 2021-2023 GI− 11220200101549CO]; Agencia Nacional de Promoción Científica y Tecnológica (ANPCyT) [PICT-2021- I-A-00328] and Universidad de Buenos Aires [UBACyT 2023-2025 - 20020220300232BA].

Data Availability Statement: All the generated data are compiled and given in MS or Supplementary files. The raw data will be provided upon reasonable request.

AI statement: The latest version of ChatGPT (GPT-5 mini) was used solely for grammar and language review in this manuscript.

Acknowledgments: We gratefully acknowledge Julieta Agustina Repetti, Carolina Verónica Vecino and Veronica Boggio for their valuable assistance with PJ collection in the rat model.

Conflicts of Interest: The authors declare no conflict of interest.

Figure legends

Figure 1. VMP1 is secreted into the cell culture medium via EVs. (**A**) Detection of CD63 in the VMP1.GFP-EV fraction by immunoblotting. (**B**) Immunoblot analysis of WCLs and EV fractions isolated by ultracentrifugation from HEK293T cells transfected with VMP1.GFP or empty GFP control. Membranes were probed with an anti-GFP antibody. (**C**) Representative confocal microscopy images of VMP1.GFP–positive EVs purified from conditioned medium (CM) of HEK293T cells transfected with VMP1.GFP for 48 h. Scale bars: 15 μm (overview),

1 μm (zoomed image). (**D**) Quantification of GFP fluorescence intensity (FI) in the VMP1.GFP-EV fraction compared to the empty GFP-EV fraction. Data are representative of n = 5 biologically independent experiments for panels A–D, and n = 3 for panel F. (**E**) Immunoblot analysis of VMP1.FLAG in WCLs and EVs from HEK293T cells using the antibody against FLAG. (**F**) Detection of VMP1.V5 in WCLs and EVs from HEK293T cells by immunoblotting using anti-V5.

Figure 2. VMP1 is localized to the membrane of VMP1-EVs. (**A**) Immunoblot analysis with anti-GFP of VMP1.GFP EVs either untreated or treated with 100 μg/mL trypsin, with or without 1% Triton X-100 (TX-100), for 30 minutes at 37 °C. TX-100 was used as a positive control for trypsin accessibility. Protease sensitivity was assessed to determine membrane association of VMP1. Representative data from *n* = 3 biologically independent experiments are shown. (**B**) Representative TEM image of VMP1.FLAG–positive EVs isolated from the CM of HEK293T cells and purified by immunoprecipitation using anti-FLAG magnetic beads. Vesicles range in size from 150 to 200 nm. Scale bar: 50 nm. (**C**) Violin plot showing the size distribution of VMP1.FLAG-EVs based on TEM measurements (*n* = 25 vesicles). (**D**) DLS profile showing the intensity-based size distribution of VMP1.FLAG-EVs purified from CM (*n* = 3 biologically independent experiments).

Figure 3. VMP1-EVs are internalized by the recipient cell. (**A**) Representative confocal images of HeLa cells incubated overnight with VMP1.GFP–positive extracellular vesicles. Internalized EVs were visualized via direct GFP fluorescence. Scale bar: 10 μm (**B**) Z-stack confocal images of AR42J pancreatic acinar cells following overnight incubation with VMP1.FLAG–positive EVs. Cells were immunostained with anti-FLAG and anti–α-tubulin antibodies; nuclei were counterstained with DAPI. Scale bar: 10 μm. (**C**) Representative confocal images of HeLa cells immunolabeled with anti-LC3 after overnight incubation with

Empty GFP-EVs or VMP1.GFP-EVs. The bar chart shows the mean ± SD of LC3 dots per cell, quantified from more than 40 cells across 3 independent experiments. ***$p < 0.001$, Mann–Whitney test. Scale bar: 10 µm.

Figure 4. VMP1 Secretion is Dependent on Autophagy. (**A**) HEK293T cells transfected with VMP1.FLAG were treated for 16 h with either starvation medium (STV) or the mTOR inhibitor PP242 (1 µM). Immunoblot analysis of WCL was performed using antibodies against FLAG, LC3, and actin (loading control). EV fractions were analyzed by immunoblotting with anti-FLAG to detect secreted VMP1.FLAG. The bar chart shows the mean ± SEM of VMP1.FLAG levels in EVs, normalized to VMP1.FLAG levels in WCL relative to actin. Data represent mean ± SEM from n = 3 biologically independent experiments. Statistical analysis was performed using one-way ANOVA; *$p < 0.01$ versus control. (**B**) HEK293T cells transfected with VMP1.FLAG were treated with chloroquine (CQ, 50 µM) for 16 h to block autophagic flux. Immunoblot analysis of WCL was performed against FLAG, LC3, and actin (loading control). EV fractions were analyzed by immunoblotting with anti-FLAG to detect VMP1.FLAG. The bar chart shows the mean ± SEM of VMP1.FLAG levels in EVs, normalized to VMP1-FLAG levels in WCL relative to actin. Data represent mean ± SEM from n = 3 biologically independent experiments. Statistical significance was determined using one-way ANOVA; *$p < 0.01$ versus control. (**C**) Confocal images of HeLa cells transfected overnight with VMP1.GFP or VMP1$^{\Delta Atg}$.GFP. Direct GFP fluorescence was used to visualize protein localization. Scale bar: 10 µm. (**D**) HEK293T cells transfected with VMP1.GFP or VMP1$^{\Delta Atg}$.GFP. Immunoblot analysis of WCL with anti-GFP and anti-actin (loading control) and of EV fractions with anti-GFP. (**E**) HEK293T cells transfected with VMP1.FLAG were treated overnight with BafA1 (10 nM; 16 h). EVs were immunoprecipitated using anti-FLAG magnetic beads, followed by immunoblot analysis for FLAG and LC3. (**F**) Immunoblot analysis of WCL and EV fractions from HEK293T cells co-transfected with FLAG-Ub and

either empty-GFP or VMP1.GFP. Immunoprecipitation was performed using magnetic beads conjugated with anti-GFP, followed by immunoblotting for VMP1 (N-terminal) and FLAG. The VMP1 immunoblot shows multiple bands above 73 kDa in eluates from both total lysates and EVs, consistent with ubiquitinated VMP1.

Figure 5. Endogenous VMP1 Secretion Requires Autophagosome Formation and Is Induced by Lysosomal inhibition. (**A**) VMP1 is detected in EVs independently of ATG5. EVs were isolated from wild-type (WT) and *Atg5* knockout (*Atg5* KO) mouse embryonic fibroblasts (MEFs) either untreated or treated with BafA1 (100 nM, 16 h). Immunoblot analysis of EV and WCL fractions was performed using antibodies against VMP1 (C-terminal) and LC3. ATG5 and actin were used as genotype and loading controls, respectively, in WCLs. The bar chart shows the mean ± SEM of VMP1 levels in EVs, normalized to VMP1 levels in WCL relative to actin. Data represent mean ± SEM (n = 3 independent experiments). Statistical analysis was performed using two-way ANOVA; *$p < 0.05$, **$p < 0.01$, ***$p < 0.001$. (**B**) MIA PaCa-2 cells with stable *VMP1* KD (shVMP1) were treated overnight with BafA1 (20 nM, 16 h). WCL and EV fractions were analyzed by immunoblot for p62, VMP1 (N-terminal), LC3, and actin (loading control for WCL). (**C**) The bar chart shows the mean and SEM of LC3-II levels in EVs, normalized to LC3-II in WCL and actin, relative to control. $p < 0.05$ by Welch's t-test vs. control. n= 3 independent experiments. (**D**) The bar chart shows the mean and SEM of p62 levels in EVs, normalized to p62 in WCL and actin, relative to control. $p < 0.05$ by Welch's t-test vs. control. n= 3 independent experiments.

Figure 6. VMP1 Secretion Is Upregulated in Pancreatic Acinar Cells under Lysosomal Stress and Experimental Acute Pancreatitis. (**A**) AR42J cells were treated with BafA1 (20 nM, 16 h) or left untreated. Immunoblot analysis of WCLs and extracellular vesicle (EV) fractions was performed to detect VMP1 (C-terminal), p62, and LC3. Actin was used as a loading control for WCLs. The bar chart shows the mean ± SEM of VMP1 levels in EVs, normalized to VMP1

levels in WCL relative to actin. Bars represent the mean ± SEM from three independent experiments. Statistical analysis was performed using Welch's t-test; **$p < 0.01$. (**B**) Cellular model of AP: AR42J cells were treated with caerulein (CAE, 7.4 µM, 16 h) or left untreated. Immunoblot analysis of WCLs and EV fractions was performed using anti-VMP1 (C-terminal) and anti-LC3 to assess VMP1 and LC3 levels in EV fractions. Actin was used as a loading control for WCLs. Bar charts show mean ± SEM of LC3-II and VMP1 in EVs, normalized to WCL levels of the same protein relative to actin. $p < 0.05$ by Welch's t-test vs. control. n= 3 independent experiments. Bars represent the mean ± SEM from three independent experiments. Statistical analysis was performed using Welch's t-test; *$p < 0.05$. (**C**) Animal model of AP: Immunoblot of VMP1 using anti-VMP1 (C-terminal) in the EV fraction obtained from PJ of rats treated with Arg or physiological solution (PS). The graph shows the quantification of VMP1 levels relative to the control. **: $p < 0.01$ by unpaired t-test vs. control. n = 5 for PS group, n = 4 for Arg group.

Figure 7. Proposed model of VMP1-EV release in SA responses to stress. Schematic model. VMP1 is secreted as a membrane component of extracellular EVs, ubiquitinated, with its C-terminal domain exposed on the outer surface. VMP1-EVs also contain LC3-II and are mainly 110–190 nm in diameter. VMP1-EV secretion depends on ATG5, is decreased by mTOR inhibition (via starvation or PP242 treatment), and is increased under lysosomal blockade (via chloroquine or BafA1). VMP1 is involved in LC3 and p62 secretion. Figure created with Biorender.com.

Figure 8. Schematic model of VMP1-EV release during pancreatitis. VMP1 is secreted in EVs into PJ, with levels markedly increased upon pancreatitis induction. Figure created with Biorender.com.

References

[1] Klionsky DJ, Abdel-Aziz AK, Abdelfatah S, et al. Guidelines for the use and interpretation of assays for monitoring autophagy (4th edition)1. Autophagy. 2021;17(1):1–382.

[2] Ponpuak M, Mandell MA, Kimura T, et al. Secretory autophagy [Internet]. Current Opinion in Cell Biology. Elsevier Ltd; 2015. p. 106–116. Available from: http://dx.doi.org/10.1016/j.ceb.2015.04.016.

[3] Leidal AM, Huang HH, Marsh T, et al. The LC3-conjugation machinery specifies the loading of RNA-binding proteins into extracellular vesicles. Nat Cell Biol. 2020;22(2):187–199.

[4] Welsh JA, Goberdhan DCI, O'Driscoll L, et al. Minimal information for studies of extracellular vesicles (MISEV2023): From basic to advanced approaches. J Extracell Vesicles. 2024;13(2):e12404.

[5] Kumar MA, Baba SK, Sadida HQ, et al. Extracellular vesicles as tools and targets in therapy for diseases. Signal Transduct Target Ther. 2024;9(1):27.

[6] Koenig U, Fobker M, Lengauer B, et al. Autophagy facilitates secretion and protects against degeneration of the Harderian gland. Autophagy. 2015;11(2):298–313.

[7] Solvik TA. Endolysosomal Inhibition Induces the Autophagy-Dependent Secretion of Autophagosomal Cargo. 2020.

[8] Urano Y, Mori C, Fuji A, et al. 6-Hydroxydopamine induces secretion of PARK7/DJ-1 via autophagy-based unconventional secretory pathway. Autophagy. 2018;14(11):1943–1958.

[9] Jahangiri B, Saei AK, Obi PO, et al. Exosomes, autophagy and ER stress pathways in human diseases: Cross-regulation and therapeutic approaches. Biochim Biophys Acta Mol Basis Dis. 2022;1868(10):166484.

[10] Dusetti NJ, Jiang Y, Vaccaro MI, et al. Cloning and expression of the rat vacuole membrane protein 1 (VMP1), a new gene activated in pancreas with acute pancreatitis, which promotes vacuole formation. Biochem Biophys Res Commun. 2002;290(2):641–649.

[11] Ropolo A, Grasso D, Pardo R, et al. The pancreatitis-induced vacuole membrane protein 1 triggers autophagy in mammalian cells. J Biol Chem. 2007;282(51):37124–37133.

[12] Molejon MI, Ropolo A, Re AL, et al. The VMP1-Beclin 1 interaction regulates autophagy induction. Sci Rep [Internet]. 2013;3.

[13] Nascimbeni AC, Giordano F, Dupont N, et al. ER –plasma membrane contact sites contribute to autophagosome biogenesis by regulation of local PI 3P synthesis. EMBO J. 2017;36(14):2018–2033.

[14] Renna FJ, Enriqué Steinberg JH, Gonzalez CD, et al. Ubiquitination Is a Novel Post-

Translational Modification of VMP1 in Autophagy of Human Tumor Cells. Int J Mol Sci [Internet]. 2023;24(16).

[15] Vaccaro MI, Grasso D, Ropolo A, et al. VMP1 expression correlates with acinar cell cytoplasmic vacuolization in arginine-induced acute pancreatitis. Pancreatology. 2003;3(1):69–74.

[16] Lo Ré AE, Fernández-Barrena MG, Almada LL, et al. Novel AKT1-GLI3-VMP1 pathway mediates KRAS oncogene-induced autophagy in cancer cells. J Biol Chem. 2012;287(30):25325–25334.

[17] Gilabert M, Vaccaro MI, Fernandez-Zapico ME, et al. Novel role of VMP1 as modifier of the pancreatic tumor cell response to chemotherapeutic drugs. J Cell Physiol. 2013;228(9):1834–1843.

[18] Ropolo A, Catrinacio C, Renna FJ, et al. A Novel E2F1-EP300-VMP1 Pathway Mediates Gemcitabine-Induced Autophagy in Pancreatic Cancer Cells Carrying Oncogenic KRAS. Front Endocrinol . 2020;11(June):1–14.

[19] Grasso D, Sacchetti ML, Bruno L, et al. Autophagy and VMP1 expression are early cellular events in experimental diabetes. Pancreatology. 2009;9(1-2):81–88.

[20] Grasso D, Ropolo A, Lo Ré A, et al. Zymophagy, a novel selective autophagy pathway mediated by VMP1-USP9x-p62, prevents pancreatic cell death. J Biol Chem. 2011;286(10):8308–8324.

[21] Vanasco V, Ropolo A, Grasso D, et al. Mitochondrial Dynamics and VMP1-Related Selective Mitophagy in Experimental Acute Pancreatitis. 2021;9(March):1–16.

[22] Boggio V, Gonzalez CD, Zotta E, et al. VMP1 Constitutive Expression in Mice Dampens Pancreatic and Systemic Histopathological Damage in an Experimental Model of Severe Acute Pancreatitis. Int J Mol Sci [Internet]. 2025;26(7).

[23] Renna FJ, Herrera Lopez M, Manifava M, et al. Evaluating Autophagy Levels in Two Different Pancreatic Cell Models Using LC3 Immunofluorescence. J Vis Exp [Internet]. 2023;(194). doi: 10.3791/65005.

[24] Buratta S, Tancini B, Sagini K, et al. Lysosomal exocytosis, exosome release and secretory autophagy. Int J Mol Sci. 2020;21(2576):1–20.

[25] Solvik TA, Nguyen TA, Lin Y-HT, et al. Autophagy cargo receptors are secreted via extracellular vesicles and particles in response to endolysosomal inhibition or impaired autophagosome maturation [Internet]. bioRxiv. bioRxiv; 2021. Available from: http://biorxiv.org/lookup/doi/10.1101/2021.08.12.456045.

[26] Pallet N, Sirois I, Bell C, et al. A comprehensive characterization of membrane vesicles released by autophagic human endothelial cells. Proteomics. 2013;13(7):1108–1120.

[27] Sirois I, Groleau J, Pallet N, et al. Caspase activation regulates the extracellular export of autophagic vacuoles. Autophagy. 2012;8(6):927–937.

[28] Hessvik NP, Øverbye A, Brech A, et al. PIKfyve inhibition increases exosome release

and induces secretory autophagy. Cell Mol Life Sci. 2016;73(24):4717–4737.

[29] Yanez-Mo M, Siljander PR-M, Nazarenko I, et al. Biological Properties of Extracellular Vesicles and Their Physiological Functions. 2015.

[30] Cocozza F, Grisard E, Martin-Jaular L, et al. SnapShot: Extracellular Vesicles. Cell. 2020;182(1):262–262.e1.

[31] Zou W, Lai M, Zhang Y, et al. Exosome Release Is Regulated by mTORC1. Adv Sci. 2019;6(3):1801313.

[32] Bhat OM, Yuan X, Kukreja RC, et al. Regulatory role of mammalian target of rapamycin signaling in exosome secretion and osteogenic changes in smooth muscle cells lacking acid ceramidase gene. FASEB J. 2021;35(7):e21732.

[33] Ortega FG, Roefs MT, de Miguel Perez D, et al. Interfering with endolysosomal trafficking enhances release of bioactive exosomes. Nanomedicine. 2019;20:102014.

[34] Xu J, Yang KC, Go NE, et al. Chloroquine treatment induces secretion of autophagy-related proteins and inclusion of Atg8-family proteins in distinct extracellular vesicle populations. Autophagy. 2022;18(11):2547–2560.

[35] Cashikar AG, Hanson PI. A cell-based assay for CD63-containing extracellular vesicles. PLoS One. 2019;14(7):e0220007.

[36] Villarroya-Beltri C, Baixauli F, Mittelbrunn M, et al. ISGylation controls exosome secretion by promoting lysosomal degradation of MVB proteins. Nat Commun. 2016;7:13588.

[37] Noh SH, Gee HY, Kim Y, et al. Specific autophagy and ESCRT components participate in the unconventional secretion of CFTR. Autophagy. 2018;14(10):1761–1778.

[38] Guo H, Chitiprolu M, Roncevic L, et al. Atg5 Disassociates the V1V0-ATPase to Promote Exosome Production and Tumor Metastasis Independent of Canonical Macroautophagy. Dev Cell. 2017;43(6):716–730.e7.

[39] Zahoor M, Farhan H. Crosstalk of Autophagy and the Secretory Pathway and Its Role in Diseases. Int Rev Cell Mol Biol. 2018;337:153–184.

[40] Gonzalez CD, Resnik R, Vaccaro MI. Secretory Autophagy and Its Relevance in Metabolic and Degenerative Disease. Front Endocrinol (Lausanne). 2020;11:266.

[41] Hegyi P, Rakonczay Z Jr, Sári R, et al. L-arginine-induced experimental pancreatitis. World J Gastroenterol. 2004;10(14):2003–2009.

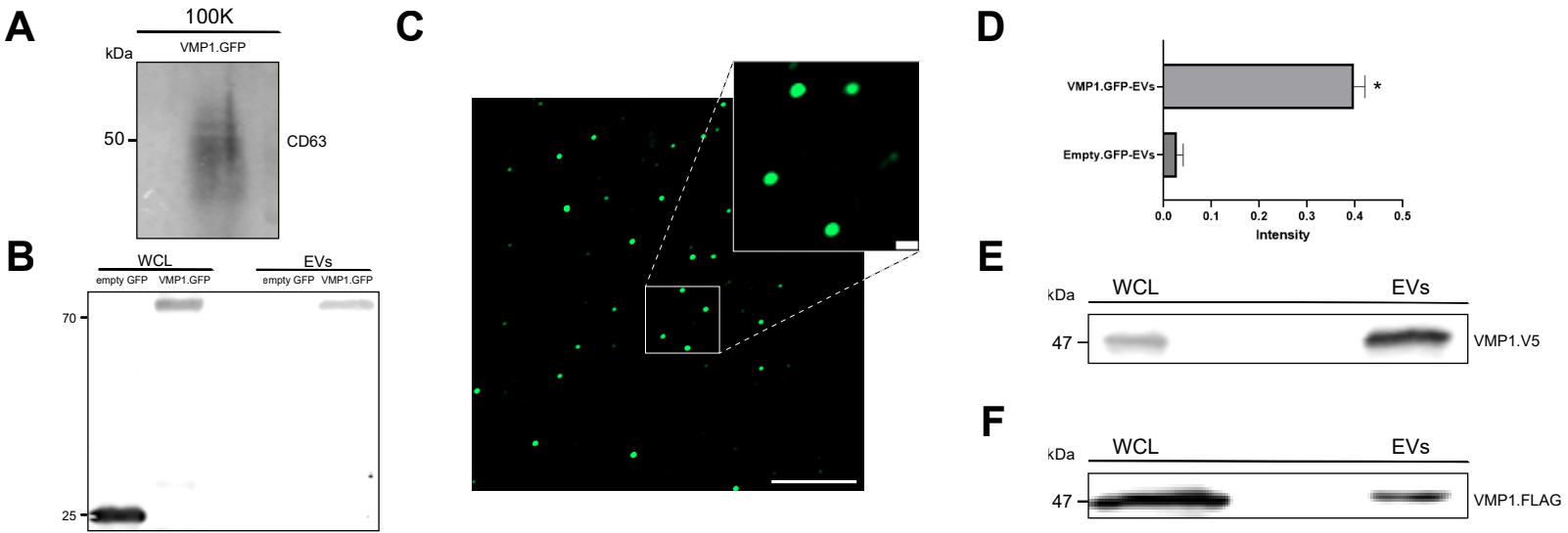
A
100K
kDa
VMP1.GFP
50
CD63
B
WCL
EVs
empty GFP
VMP1.GFP
empty GFP
VMP1.GFP
70
25
C
D
VMP1.GFP-EVs
Empty.GFP-EVs
*
0.0
0.1
0.2
0.3
0.4
0.5
Intensity
E
kDa
WCL
EVs
47
VMP1.V5
F
kDa
WCL
EVs
47
VMP1.FLAG

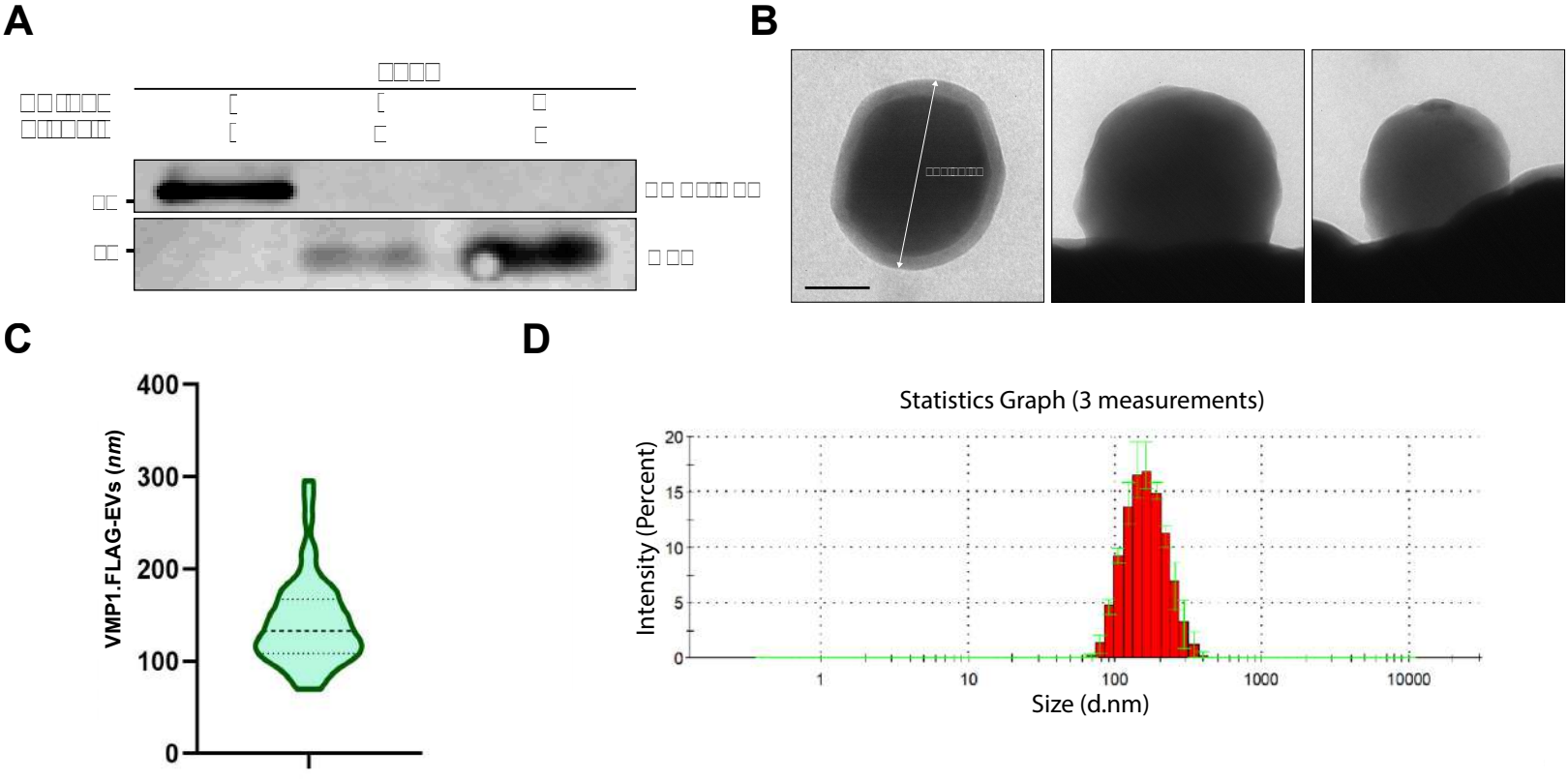
A
B
C
D
VMP1.FLAG-EVs (nm)
400
300
200
100
0
Statistics Graph (3 measurements)
Intensity (Percent)
20
15
10
5
0
1
10
100
1000
10000
Size (d.nm)

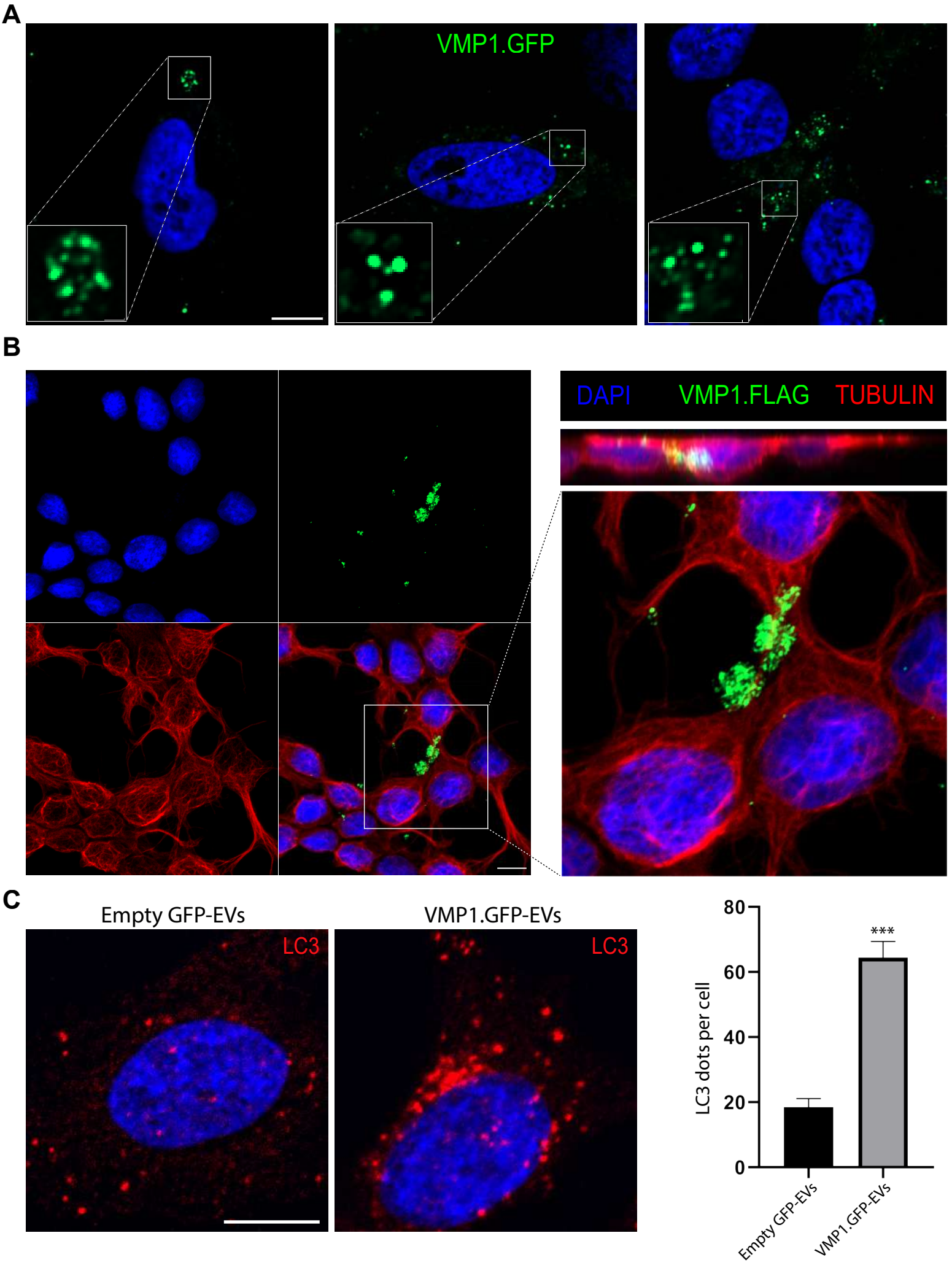
A
VMP1.GFP
B
DAPI
VMP1.FLAG
TUBULIN
C
Empty GFP-EVs
VMP1.GFP-EVs
LC3
LC3
LC3 dots per cell
80
60
40
20
0
***
Empty GFP-EVs
VMP1.GFP-EVs

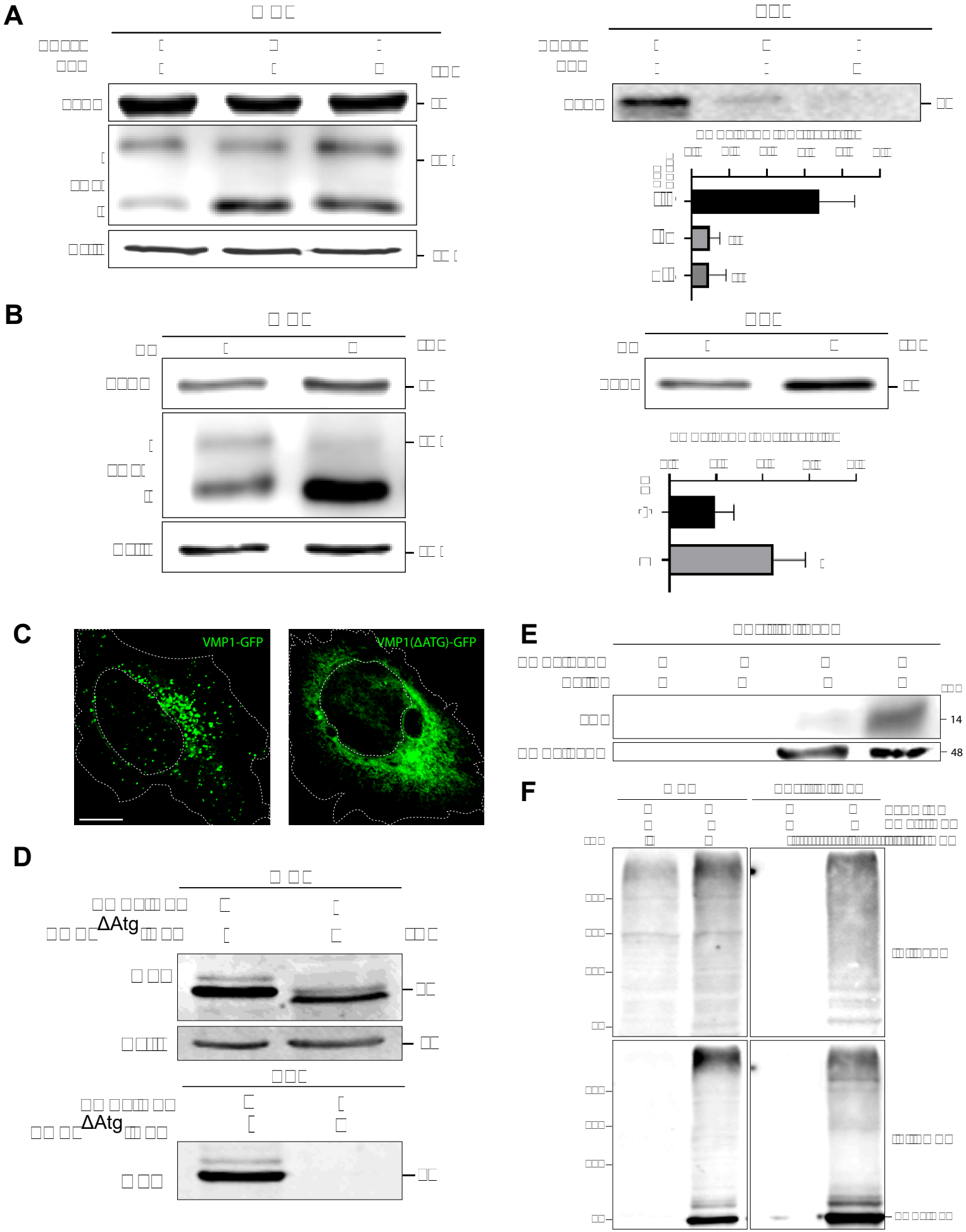
A
B
C
VMP1-GFP
VMP1(ΔATG)-GFP
D
ΔAtg
ΔAtg
E
14
48
F

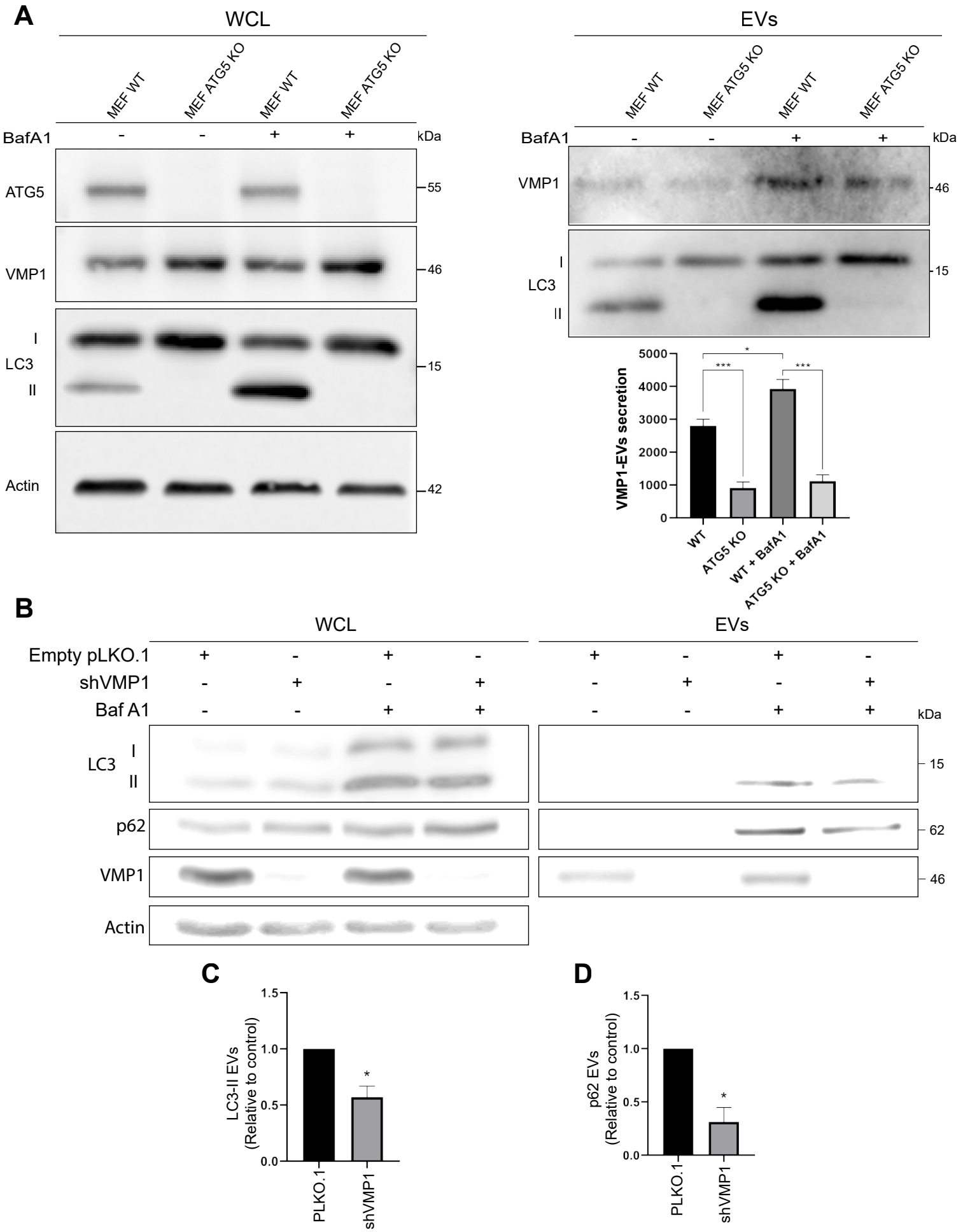
A
WCL
EVs
MEF WT
MEF ATG5 KO
MEF WT
MEF ATG5 KO
BafA1
- - + +
kDa
ATG5
55
VMP1
46
I
LC3
II
15
Actin
42
VMP1
46
I
LC3
II
15
VMP1-EVs secretion
5000
4000
3000
2000
1000
0
*
***
***
WT
ATG5 KO
WT + BafA1
ATG5 KO + BafA1
B
WCL
EVs
Empty pLKO.1
shVMP1
Baf A1
LC3
I
II
p62
VMP1
Actin
15
62
46
C
LC3-II EVs
(Relative to control)
1.5
1.0
0.5
0.0
*
PLKO.1
shVMP1
D
p62 EVs
(Relative to control)
1.5
1.0
0.5
0.0
*
PLKO.1
shVMP1

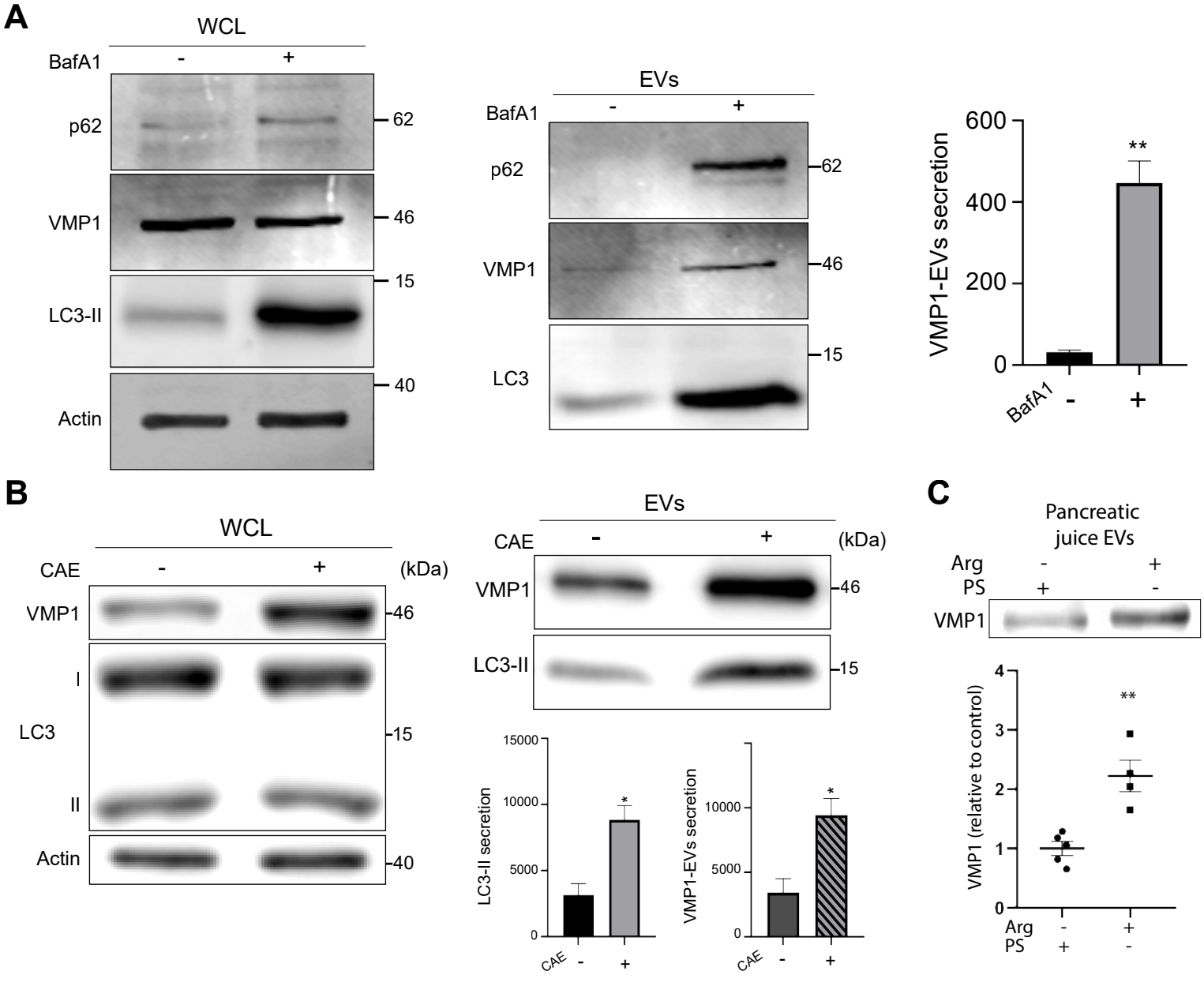
A
WCL
BafA1
-
+
p62
VMP1
LC3-II
Actin
62
46
15
40
EVs
BafA1
-
+
p62
VMP1
LC3
62
46
15
VMP1-EVs secretion
600
400
200
0
**
BafA1
-
+
B
WCL
CAE
-
+
(kDa)
VMP1
I
LC3
II
Actin
46
15
40
EVs
CAE
-
+
(kDa)
VMP1
LC3-II
46
15
LC3-II secretion
15000
10000
5000
0
*
CAE
-
+
VMP1-EVs secretion
10000
5000
0
*
CAE
-
+
C
Pancreatic
juice EVs
Arg
PS
-
+
+
-
VMP1
VMP1 (relative to control)
4
3
2
1
0
**
Arg
PS
-
+
+
-

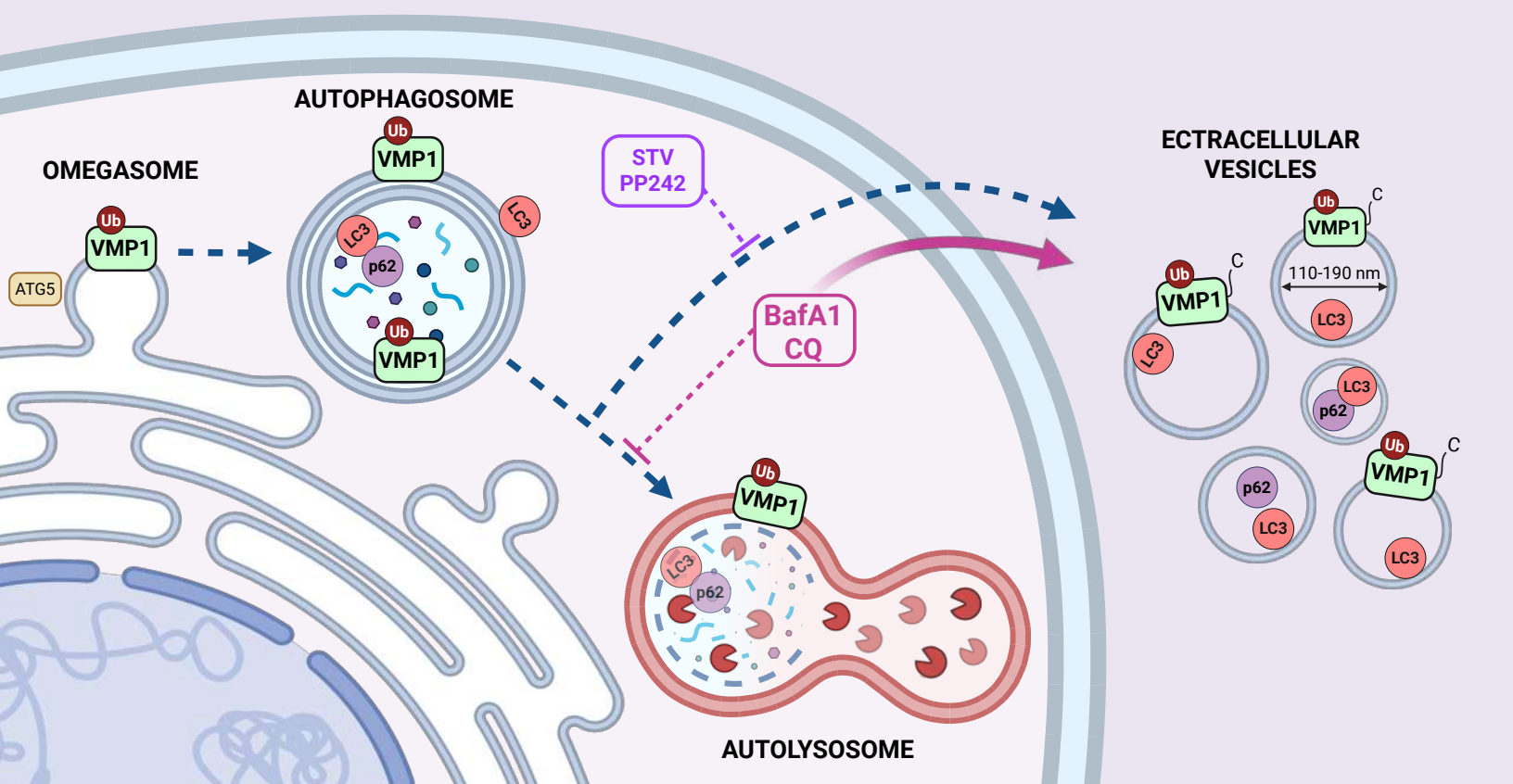
OMEGASOME
Ub
VMP1
ATG5
AUTOPHAGOSOME
Ub
VMP1
LC3
LC3
p62
Ub
VMP1
STV
PP242
BafA1
CQ
Ub
VMP1
LC3
p62
AUTOLYSOSOME
ECTRACELLULAR
VESICLES
Ub
VMP1
C
LC3
Ub
VMP1
C
110-190 nm
LC3
LC3
p62
p62
LC3
Ub
VMP1
C
LC3

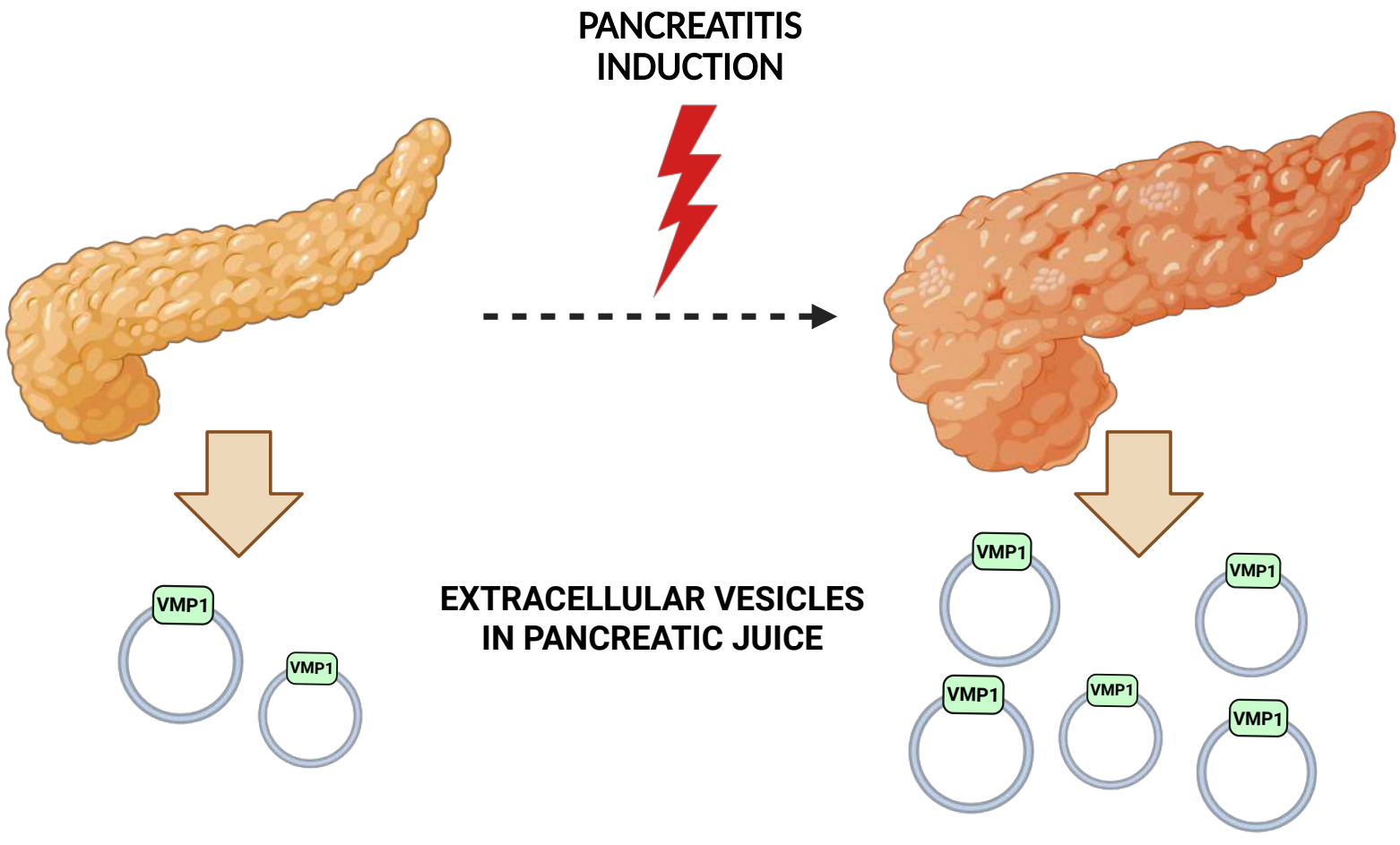
PANCREATITIS
INDUCTION
VMP1
VMP1
EXTRACELLULAR VESICLES
IN PANCREATIC JUICE
VMP1
VMP1
VMP1
VMP1
VMP1